Applied Ocean Research (2013)

Contents lists available at ScienceDirect

Applied Ocean Research

journal homepage: www.elsevier.com/locate/apor

Multibody dynamics of floating wind turbines with large-amplitude motion

Lei Wang*, Bert Sweetman[1]

Texas A&M University, Department of Civil Engineering, College Station, TX 77843-3136, United States

ARTICLE INFO

Article history:
Received 26 June 2012
Received in revised form 16 May 2013
Accepted 28 June 2013

Keywords:
Floating wind turbines
Large-amplitude motion
Conservation of momentum
Multibody dynamics
Simulation
Euler angles

ABSTRACT

A new approach to multibody dynamics is investigated by treating floating wind turbines as multibody systems. The system is considered as three rigid bodies: the tower, nacelle and rotor. Three large-amplitude rotational degrees of freedom (DOFs) of the tower are described by 1-2-3 sequence Euler angles. Translation of the entire system is described by Newton's second Law applied to the center of mass (CM) of the system and transferred to 3 translational DOFs of the tower. Additionally, two prescribed DOFs governed by mechanical control, nacelle yaw and rotor spin, are combined with the 6 DOFs of the tower to formulate the 8-DOF equations of motion (EOMs) of the system. The CM of the system is generally time-varying and not constrained to any rigid body due to the arbitrary location of the CM of each body and relative mechanical motions among the bodies. The location of the CM being independent of any body is considered in both the solution to 3 translational DOFs and the calculation of angular momentum of each body for 3 rotational DOFs. The theorem of conservation of momentum is applied to the entire multibody system directly to solve 6 unknown DOFs. Motions computed using the six nonlinear EOMs are transformed to each body in a global coordinate system at every time-step for use in the computation of hydrodynamics, aerodynamics and restoring forcing, which preserves the nonlinearity between external excitation and structural dynamics. The new method is demonstrated by simulation of the motion of a highly compliant floating wind turbine. Results are verified by critical comparison with those of the popular wind turbine dynamics software FAST.

1. Introduction and background

Use of floating structures to support large utility-scale wind turbines is likely remaining as a viable contender for future offshore wind farm developments. The primary benefit of floating structures is that they can be sited in very deep waters that may be beyond sight from land; one primary drawback is cost. Design bases requiring the tower to remain nearly vertical in the presence of strong wind forces increase support structure cost because the required buoyancy far exceeds the weight of the equipment being supported. Savings could potentially be realized by reducing hull size, with the design trade-off of allowing more compliance with the wind thrust force in the pitch direction.

Design of these increasingly compliant floating towers will make computation of structural dynamics both more challenging and more important. Specific design challenges associated with large rotations include: gyroscopic moments, potential loss of effective swept area and consideration of inertial loading. Gyroscopic moments for conventional, stiff, bottom-founded structures are primarily generated by mechanical precession of the spin axis to adapt to shifting winds, and so are limited by the maximum yaw rate [1]. However, no such limit exists for gyroscopic moments of floating structures because they result from both shifting winds and irregular motions of the tower. Large pitch angles reduce the effective blade swept area perpendicular to the wind, but this effect has been shown to have only a modest effect on energy capture [2]. Intuition may suggest that increased dynamic motions correspond to increased dynamic loading, but in some cases reduced stiffness actually lowers dynamic loading. For sinusoidal motion, the amplitude of the inertial loads is the product of the moment of inertia, amplitude of the motion and the square of the circular frequency. Decreasing the stiffness reduces the pitch and roll natural frequencies, which decreases inertial loading, but may require special consideration in the design of the rotor speed and blade-pitch controllers. Rigorous design of these new concepts requires use of accurate and efficient simulation methodologies. Here, simulation of rigid-body dynamics using a reduced set of only 6 EOMs enables very rapid time-domain simulation, though vibration and fatigue associated with member flexibility cannot be captured. Neglecting the structural flexibility of individual bodies is reasonable in cases where global motions are of primary interest and the motion allowed by compliance between members is much larger than that allowed by the structure stiffness of each member.

[1] Present address: Texas A&M University, Maritime Systems Engineering Department, 200 Seawolf Parkway, Galveston, TX 77553-1675, United States.

* Corresponding author. Present address: Texas A&M University, Maritime Systems Engineering Department, 200 Seawolf Parkway, Galveston, TX 77553-1675, United States. Tel.: +1 409 740 4834; fax: +1 409 741 7153.

E-mail addresses: lei.ray@hotmail.com (L. Wang) sweetman@tamu.edu (B. Sweetman).

0141-1187/$ - see front matter © 2013 Elsevier Ltd. All rights reserved.
http://dx.doi.org/10.1016/j.apor.2013.06.004

Multibody system analysis can be used to simulate a complex system made up of rigid bodies connected by mechanical joints. A compliant floating wind turbine system can be considered as a multibody system including tower, rotor, nacelle and other moving parts, which are mechanically connected by the yaw bearing, hub, etc. One conventional analytical method to simulate the dynamics motions of such a system is the Newton–Euler (NE) equations or Euler–Lagrange (EL) equations [3]. The NE equations are usually established by separating the free-body diagrams of each rigid body in the system. For example, Featherstone [4] applies various NE algorithms to a rigid-body system with a floating base body. Dynamics of robots are systematically solved by Mason using NE method [5]. Stoneking [6] presents the derivation of the exact nonlinear dynamic equations of motion for a multibody spacecraft connected by spherical gimbal joints. Of special relevance to this work, Matsukuma and Utsunomiya [7] employ NE equations combined with constraint conditions associated with the joints between rigid bodies to analyze the dynamic response of a 2-MW downwind turbine mounted on a spar-type floating platform for pitch amplitudes up to around 10 degrees in steady wind, but no waves, and conclude that the platform motions are meaningfully influenced by gyro moments associated with rotor rotation. The EL equations apply energy methods to establish equations of motion for generalized degrees of freedom. Overall, the commonly used NE method computes the internal forcing between rigid bodies, and is excellent for the applications in which internal forces are the primary concern. However, for simulation of general motion of a system, these internal forces are not needed and impose an unnecessary computational burden. The EL method is efficient for the solution of motion if internal forces are not needed, but the necessary derivation of partial derivatives of energy about related generalized DOFs can be laborious. Both the NE and EL methods require solution of a number of coupled equations equal to that of DOFs. The number of equations of the NE method is six times the number of rigid bodies within the system; the number of equations for the EL method is just that of the generalized DOFs, which is generally much greater than six. One alternative is Kane's method, which combines the advantages of both the NE and EL methods. Kane's method is employed in the well-recognized wind turbine dynamics analysis software, the NREL FAST aero-elastic simulator [8,9]. FAST is highly developed and well recognized, and includes the option of computing hydrodynamic radiation-diffraction analysis package WAMIT [10]. WAMIT relies on small-amplitude assumptions including the conventional assumptions in radiation-diffraction theory, one of which is computation of hydrostatic restoring forces with the floating body at a fixed position. The solution technique in FAST is consistent with these wave-force calculation assumptions. Subsequently, large-amplitude motions exceed present capabilities of FAST, which is limited to platform rotation of less than 20°. Kane's method is based on virtual work theory, so the flexible members can be directly included, but it also requires solving a large number of coupled differential EOMs.

A new alternative to both Kane's method and to FAST was developed by Wang and Sweetman [11], in which the EOMs are established by applying the conservation of momentum to the floating wind turbine system directly. The work presented here is a significant generalization of earlier work, while still maintaining its main advantages. In that prior work, only 6 equations are needed to describe the general motion of the 2-body system with the relative motions of nacelle yaw and rotor spin: three equations for the position of the CM of the system and another three for the large-amplitude rotation of the tower (base body). The core of the method is to calculate the angular momentum of each rigid body and sum them in a unified translating-rotating coordinate system to obtain the total angular momentum of the entire system, the derivative of which is equal to the sum of externally applied moments. One key advantage is that only six EOMs are needed regardless of how many DOFs the system has. The method directly applies the known interactions between mechanical components, i.e. nacelle yaw and rotor spin. Mechanical systems with known kinematic relationships between components are common, especially in rotating machinery. Thus, the methodology is broadly applicable to various types of interconnected dynamic mechanical systems.

In that prior work, the 2-body system was configured with the CM of the nacelle centered above the axis of the tower, such that the CM of the system remained at a fixed point on the tower axis, regardless of nacelle yaw. However, the CM of each body may be arbitrarily located, and relative motion among bodies generally changes the CM of a multibody system. Modern turbines are generally configured with the CM of the rotor-nacelle-assembly upwind of the centerline of the tower. Subsequently, the CM of the floating wind turbine system changes as the nacelle yaws relative to the tower. The theoretical developments presented here enable the application of the method to more realistic configurations. Application of the conservation of both the linear and angular momentum to the system enables solution for the CM of the entire system, but not for any body within the system, so the spatial relation between the CM of the system and that of each rigid body must be considered to find the motion of each body in space. The computation of the nonlinear mooring restoring forcing also requires determination of the motion of individual bodies at each time step. Additionally, velocities of each body must be determined because they directly affect the wind and wave forcing on the floating wind turbine. The computation of these aero- and hydrodynamic forces includes the motion of the body through the fluid. These motions are determined using a systems of transformation matrices that cascade between the various coordinate systems such that the full nonlinear coupling between external excitation and large-amplitude motion of the wind turbine system is preserved. Writing the EOMs about the CM of the system also decouples the translational and rotational inertial forcing, which facilitates numerical integration of the EOMs.

2. Coordinate systems

The implementation of the new method first requires the selection of a set of coordinates to unequivocally define the motion within the multibody system for use in derivation of the EOMs; coordinate selection is based on first selecting proper coordinate systems. Three rigid bodies in the system are the tower, nacelle and rotor. The tower includes the buoyant hull and is the complete structure supporting the topsides facility. The nacelle is the non-spinning part of the topsides; the rotor is the spinning part of the topsides, including the hub and blades. The rotor spin velocity is defined relative to the nacelle, and the combined nacelle and rotor mechanically yaws relative to the tower. There are two global earth-fixed coordinate systems, plus three body-fixed coordinate systems attached to each of the three bodies, plus one system-fixed coordinate system.

Fig. 1 shows both the (X, Y, Z) and the (X_M, Y_M, Z_M) systems, which are earth-fixed global coordinate systems with the origin located at the CM of the undisplaced tower and the still water level respectively. The (x_t, y_t, z_t), (x_n, y_n, z_n) and (x_r, y_r, z_r) coordinate systems are body fixed and originate at the instantaneous CM of the tower, nacelle and rotor, respectively. There is also a coordinate system for the entire system, (x_s, y_s, z_s). This system-fixed (x_s, y_s, z_s) is parallel to (x_t, y_t, z_t) and originates at the non-constraint CM of the entire system, the instantaneous change of which depends on the location of the CM of each body relative to the joints and on relative motion among the bodies.

The (X, Y, Z) system is used for the application of Newton's second Law. The (X_M, Y_M, Z_M) system is not used in calculations and is defined only to enable comparison of simulation results with those of FAST, in which the reference point is usually prescribed to be on the still water level. The body-fixed coordinate systems, (x_t, y_t, z_t), (x_n, y_n, z_n) and (x_r, y_r, z_r), are generally selected to be on the principal axes of inertia in order to simplify the calculation of angular momentum of

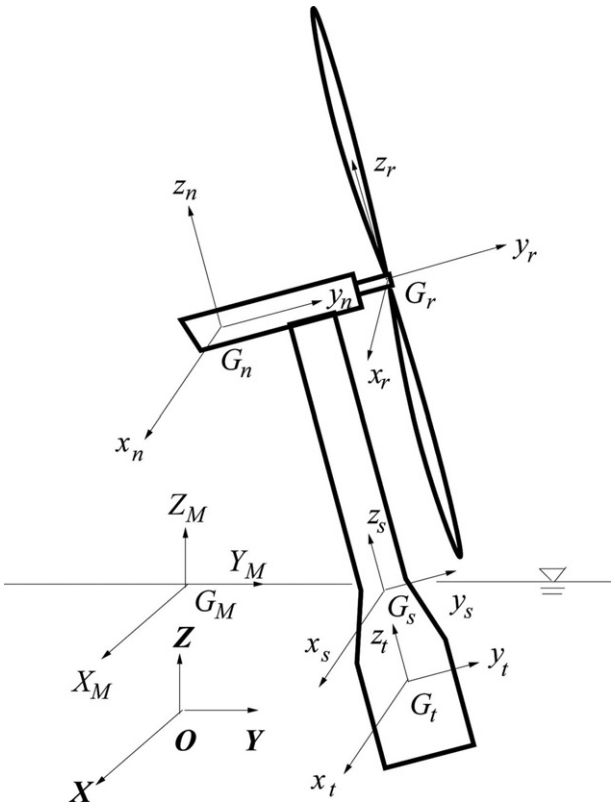

Fig. 1. Coordinate systems.

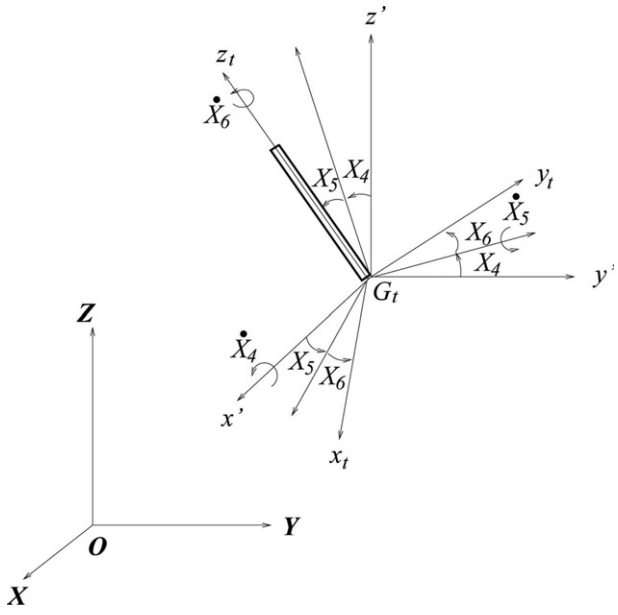

Fig. 2. 1-2-3 sequenced Euler angles in terms of X_4, X_5 and X_6.

the three rigid bodies. The system-fixed (x_s, y_s, z_s) system is used for the application of the theorem of conservation of angular momentum to the entire system. Additionally, the external excitation forces and moments applied in the dynamic equations are computed at each time step and projected into the (X, Y, Z) and (x_s, y_s, z_s) systems, respectively.

The coordinates (X_1, X_2, X_3) measured from the (X, Y, Z) system are used to define the absolute motion of the CM of the system, G_s. These coordinates are further transferred to the translations of the CM of the tower, G_t, which are notated by the coordinates (X_{1t}, X_{2t}, X_{3t}) and defined as 3 translational DOFs of the tower. Fig. 2 shows the Euler angles used to describe large-amplitude rotational motion. For large angular displacements in space, the order in which the angles of rotation are applied is important; there are 12 possible Euler angles sequences. Here, the 1-2-3 sequence of Euler angles are selected; the coordinates (X_4, X_5, X_6) denote these angles, which are 3 rotational DOFs of the tower and describe the position of the rotating tower. The (x', y', z') is a translating coordinate system with respect to the (X, Y, Z) system, with the origin located at the CM of the tower. The (x_t, y_t, z_t) system can be transformed from the (x', y', z') by: first rotating the upright tower about the x'-axis by angle X_4, and then rotating about the resulting second coordinate axis through an angle X_5, and finally, rotating the tower about the z_t-axis through the third Euler angle, X_6. Additionally, the prescribed mechanical DOFs are denoted by two relative coordinates: the vector $\vec{\omega}_{yaw}$ describes the rotation of the nacelle to the tower in the (x_t, y_t, z_t) system; the vector $\dot{\vec{\psi}}$ describes the rotation of the rotor to the nacelle (x_n, y_n, z_b) system.

3. Equations of motion of the system

Application of the conservation of momentum to the entire system eliminates the need to calculate internal forcing between contiguous rigid bodies. The conservation of angular momentum is directly applied to the entire wind turbine system to derive the rotational EOMs, and the conservation of linear momentum (Newton's second law) is applied to establish the translational EOMs. The resulting 6 EOMs of the multibody system include terms representing each of the three rigid bodies: the tower, the nacelle and the rotor. Six unknown DOFs of the tower (translation and rotation) plus two prescribed mechanical DOFs (nacelle yaw and rotor spin) are considered in the model. The EOMs of the entire system combined with coordinate transformations are used to solve the unknown general motion of the tower in the space. Tower motions and prescribed yaw and spin are then used to obtain the absolute motions of the nacelle and rotor in space.

3.1. Rotational equations of motion

Beginning with conservation of angular momentum, the sum of the moments resulting from externally applied forces about the CM of a system of particles in the translating-rotating system, (x_s, y_s, z_s), equals the change of amplitude of the angular momentum within the coordinate system plus the change of direction of the momentum with respect to global coordinate system (e.g. [12]). The rotational EOMs can be shown to be:

$$\sum \vec{M} = \left(\dot{\vec{H}}^{s}_{G_s}\right)_{x_s y_s z_s} + \vec{\omega}_s \times \vec{H}^{s}_{G_s} \tag{1}$$

where $\vec{H}^{s}_{G_s}$ is the angular momentum of the system. The form is similar to that used in the derivation of the conventional Euler dynamic equations applied to only one rigid body. A significant difference here is that the conservation of angular momentum is applied to the entire system. The single vector representing the total angular momentum in Eq. (1) is the sum of the angular momentum of each body. Summation of angular momentum of each body requires a unified coordinate system. Here, calculation of angular momentum and its derivative is greatly simplified because the translating-rotating system, (x_s, y_s, z_s), has been prescribed to be parallel to the body-fixed coordinate system (x_t, y_t, z_t). The vector $\vec{\omega}_s$ describes the angular velocity of (x_s, y_s, z_s) with respect to the global coordinate system (X, Y, Z). The left hand side of Eq. (1), $\sum \vec{M}$, represents the moments from all external forces: $\sum \vec{M} = \vec{M}_{wind} + \vec{M}_{wave} + \vec{M}_{restoring}$, where the restoring moment $\vec{M}_{restoring}$ includes the effects of both hydrostatics and

mooring lines; the environmental moments $\vec{M}_{wind}$ and $\vec{M}_{wave}$ result from wind and wave forces.

3.1.1. Calculation of angular momentum

The angular momentum of the entire system results from summing the angular momentum of each rigid body. The application of conservation of angular momentum by Eq. (1) needs the angular momentum of the complete system about the CM of the system, G_s, which can be obtained by summing up the angular momentum of each rigid body about G_s. Summing the momenta requires they be calculated about the same reference point and projected into the same coordinate system. Here, the angular momentum of each body is computed in a coordinate system through its principal axes of inertia, then transformed into the unified (x_s, y_s, z_s) system and finally transferred to the origin of the (x_s, y_s, z_s) system. Combining the first two steps, the total angular momentum of the system can be expressed by:

$$\vec{H}^s_{G_s} = \vec{H}^s + \vec{H}_{ETR} \tag{2}$$

in which the vector $\vec{H}^s$ is the total angular momentum of three bodies projected into the (x_s, y_s, z_s) system, but calculated about respective CM of each body, i.e. $\vec{H}^s = \vec{H}^s_{G_t} + \vec{H}^s_{G_n} + \vec{H}^s_{G_r}$; the term $\vec{H}_{ETR}$ represents the effect of transferring the reference point from the CM of each body to G_s. The angular momentum of each of the three rigid bodies taken about its own CM can be expressed as:

$$\begin{aligned}
\vec{H}^s_{G_t} &= T_{t\to s}\left(I_t\vec{\omega}_t\right)\\
\vec{H}^s_{G_n} &= T_{n\to s}\left(I_n\vec{\omega}_n\right)\\
\vec{H}^s_{G_r} &= T_{r\to s}\left(I_r\vec{\omega}_r\right)
\end{aligned} \tag{3}$$

where I_t, I_n and I_r are the inertia tensors of three rigid bodies, with diagonal elements equal to the moments of inertia about respective principal axes. The transformation matrix from the body-fixed coordinate system of the tower to the unified system, $T_{t\to s}$, is an identity matrix because the (x_t, y_t, z_t) system is parallel to the (x_s, y_s, z_s) system. The other two transformation matrixes about the nacelle and rotor can be shown to be (e.g. [13]):

$$\begin{aligned}
T_{n\to s}(\beta) &= \begin{bmatrix}\cos\beta & -\sin\beta & 0\\ \sin\beta & \cos\beta & 0\\ 0 & 0 & 1\end{bmatrix}\\
T_{r\to s}(\alpha) &= T_{n\to s}T_{r\to n} = T_{n\to s}\begin{bmatrix}\cos\alpha & 0 & \sin\alpha\\ 0 & 1 & 0\\ \sin\alpha & 0 & \cos\alpha\end{bmatrix}
\end{aligned} \tag{4}$$

Here, the angle α describes the relative spin of the rotor to the nacelle and is positive along the y_r-axis; the angle β describes the relative yaw of the nacelle to the tower and is positive along the z_t-axis. The absolute angular velocities in Eq. (3) are component-wise projections in the body-fixed coordinate systems of each of three bodies Wang and Sweetman [11]:

$$\begin{aligned}
\vec{\omega}_t &= \begin{bmatrix}\dot{X}_4\cos X_5\cos X_6 + \dot{X}_5\sin X_6\\ -\dot{X}_4\cos X_5\sin X_6 + \dot{X}_5\cos X_6\\ \dot{X}_4\sin X_5 + \dot{X}_6\end{bmatrix}\\
\vec{\omega}_n &= T_{t\to n}\left(\vec{\omega}_t + \vec{\omega}_{yaw}\right)\\
\vec{\omega}_r &= T_{n\to r}\left(\vec{\omega}_n + \dot{\vec{\psi}}\right)
\end{aligned} \tag{5}$$

where the vector $\vec{\omega}_{yaw}$ has positive nacelle yaw component along the z_t-direction; the spinning vector $\dot{\vec{\psi}}$ is positive along the y_r-direction. The angular momentum of the system without consideration of the transfer of reference point can be obtained by substituting Eqs. (4) and (5) into Eq. (3):

$$\begin{aligned}
\vec{H}^s &= \left(T_{t\to s}I_t + T_{n\to s}I_nT_{t\to n} + T_{r\to s}I_rT_{t\to r}\right)\vec{\omega}_t\\
&\quad + \left(T_{n\to s}I_nT_{t\to n} + T_{r\to s}I_rT_{t\to r}\right)\vec{\omega}_{yaw}\\
&\quad + T_{r\to s}I_rT_{n\to r}\dot{\vec{\psi}}
\end{aligned} \tag{6}$$

where the first bracket associated with $\vec{\omega}_t$ represents the angular momentum of the entire system in absence of the relative motion between contiguous components; the terms including the nacelle yaw rate, $\vec{\omega}_{yaw}$, and the spinning velocity, $\dot{\vec{\psi}}$, indicate the contribution of relative motion to the total angular momentum. Each of the three angular velocities is first transferred to the local coordinate systems of its rigid body to calculate the angular momentum and then transferred to the unified coordinate system (x_s, y_s, z_s), so it can be included in sum. The decreasing number of transformations for $\vec{\omega}_t$, $\vec{\omega}_{yaw}$, and $\dot{\vec{\psi}}$ is because of the cascading nature of the transformation matrix.

Eq. (6) does not include the effect of transferring the reference point, i.e. the term $\vec{H}_{ETR}$ in Eq. (2). A simple way to transfer the reference point in the calculation of angular momentum of a rigid body is to combine the angular momentum about the CM of the rigid body with the effect of the change of the reference point. For example, the angular momentum of the tower calculated about G_s can be shown to be (e.g. [12]):

$${}^t\vec{H}^s_{G_s} = \vec{H}^s_{G_t} + \vec{\rho}_{G_t/G_s}\times m_t\vec{v}_{G_t/G_s} \tag{7}$$

The cross product term in Eq. (7) is one component in $\vec{H}_{ETR}$ relative to the tower, which depends on the radius vector from G_s to G_t, $\vec{\rho}_{G_t/G_s}$, and the relative velocity of G_t to G_s, $\vec{v}_{G_t/G_s}$. The angular momenta of the nacelle and the rotor about G_s can be expressed in a form similar to Eq. (7): $\vec{H}_{ETR} = \vec{\rho}_{G_t/G_s}\times m_t\vec{v}_{G_t/G_s} + \vec{\rho}_{G_n/G_s}\times m_n\vec{v}_{G_n/G_s} + \vec{\rho}_{G_r/G_s}\times m_r\vec{v}_{G_r/G_s}$. Unknown radius vectors, $\vec{\rho}_{G_t/G_s}$, $\vec{\rho}_{G_n/G_s}$ and $\vec{\rho}_{G_r/G_s}$, need to be determined to compute the effects of the transfer of reference points.

Computing the CM of the wind turbine system also requires the spatial position of the CM of each rigid body expressed in a common coordinate system. This common system has been selected to enable significant simplification of the EOMs. Here, the body-fixed coordinate system of the base body, the (x_t, y_t, z_t) system, is chosen to measure the relative positions of the CM of each body to that of the system because it enables expressions of the locations of the tower, nacelle and rotor relative to the CM of the system as three single radius vectors, which depend on only the prescribed rotational DOFs between bodies.

First, the radius vectors from the CM of the tower (G_t) to the CM of other rigid bodies (G_n and G_r) are computed in the translating-rotating (x_t, y_t, z_t) system based on the initial configuration of the bodies and transformation matrices representing the relative rotation between the bodies. Then the CM of the system is calculated in this coordinate system to decouple the translational and rotational EOMs:

$$\begin{aligned}
\vec{\rho}_{G_n/G_t} &= \vec{\rho}_{J_n/G_t} + T_{n\to t}\vec{\rho}_{G_n/J_n}\\
\vec{\rho}_{G_r/G_t} &= \vec{\rho}_{G_n/G_t} + T_{n\to t}\vec{\rho}_{G_r/G_n}\\
\vec{\rho}_{G_t/G_s} &= -\vec{\rho}_{G_s/G_t} = -\frac{m_n\vec{\rho}_{G_n/G_t} + m_r\vec{\rho}_{G_r/G_t}}{m_t + m_n + m_r}
\end{aligned} \tag{8}$$

where m_t, m_n and m_r are the masses of the tower, nacelle and rotor, respectively. The positions of the joints measured from the proper body-fixed coordinate systems are used to relate the relative positions between the centers of mass in order to avoid the influence of spatial rotation. Here the mechanical joint J_n is located between the tower and nacelle; the radius vectors $\vec{\rho}_{J_n/G_t}$ and $\vec{\rho}_{G_n/J_n}$ are projected into the (x_t, y_t, z_t) and (x_n, y_n, z_n) systems, respectively. Both of these vectors result from the initial geometrical configuration within the

multibody system and remain constant, as shown in Fig. 1. The radius vector $\vec{\rho}_{G_r/G_n}$ can be obtained following the pattern of $\vec{\rho}_{G_n/G_t}$, i.e. $\vec{\rho}_{G_r/G_n} = \vec{\rho}_{J_r/G_n} + T_{r\to n}\vec{\rho}_{G_r/J_r}$. The CM of the nacelle and of the rotor w.r.t that of the system can be obtained by means of $\vec{\rho}_{G_t/G_s}$, e.g. $\vec{\rho}_{G_n/G_s} = \vec{\rho}_{G_n/G_t} + \vec{\rho}_{G_t/G_s}$. Importantly, that part of the angular momentum associated with the effect of the transfer of the reference point does not depend on translation of the system, which makes the inertial forcing in the rotational EOMs independent of the translational kinematics such that the 6 × 6 inertial matrix effectively becomes two full 3 × 3 matrices (one for translation and one for rotation), with the remaining 18 off-diagonal terms all zero. This inertial decoupling facilitates the numerical integration dramatically. Unfortunately, the equations of motion cannot be decoupled completely because the physics of the environmental forcing due to wind and waves and the restoring due to hydrostatics and mooring lines require consideration of combined rotational and translational displacement and velocities.

3.1.2. Calculation of derivative of angular momentum

The absolute derivative of the angular momentum of the system includes the local derivative in the unified coordinate system (x_s, y_s, z_s) (the change of magnitude of the momentum) and the rotational effect (the change of direction of the momentum) in Eq. (1). In general, the angular momentum of any system can be decomposed into any arbitrary coordinate system. Here, the (x_s, y_s, z_s) coordinate system is prescribed to be parallel to the body-fixed coordinate system of the tower, (x_t, y_t, z_t), to realize two important benefits: it eliminates the complication of computing the derivative of the angular momentum, and more importantly, it decouples the velocity terms in the inertia forcing of Eq. (1). The absolute derivative of the angular momentum of the system in Eq. (1) can be expanded to:

$$\frac{d\vec{H}^s_{G_s}}{dt} = \left(\dot{\vec{H}}^s_{G_s}\right)_{x_s y_s z_s} + \vec{\omega}_s \times \vec{H}^s_{G_s} \tag{9}$$

in which

$$\vec{H}^s_{G_s} = \vec{H}^s + \vec{\rho}_{G_t/G_s} \times m_t \vec{v}_{G_t/G_s} + \vec{\rho}_{G_n/G_s} \times m_n \vec{v}_{G_n/G_s} + \vec{\rho}_{G_r/G_s} \times m_r \vec{v}_{G_r/G_s} \tag{10}$$

where the notation $(\dot{\ })_{x_s y_s z_s}$ represents the local derivative within the (x_s, y_s, z_s) system, i.e. the time change of the magnitude of the vector. The angular velocity of the (x_s, y_s, z_s) system, $\vec{\omega}_s$, is equal to rotational velocity of the tower in Eq. (5). The local derivative of the vector $\vec{H}^s$ can be obtained by directly taking the derivative of Eq. (6), which includes taking the derivative of the transformation matrixes and the angular velocities. The derivatives of the three cross product terms in Eq. (10) merit further investigation. The term associated with the tower is shown as an example:

$$\begin{aligned}
\vec{v}_{G_t/G_s} &= \frac{d\vec{\rho}_{G_t/G_s}}{dt} = \left(\dot{\vec{\rho}}_{G_t/G_s}\right)_{x_s y_s z_s} + \vec{\omega}_s \times \vec{\rho}_{G_t/G_s} \\
\left(\dot{\vec{\rho}}_{G_t/G_s} \times m_t \vec{v}_{G_t/G_s}\right)_{x_s y_s z_s} &= \vec{\rho}_{G_t/G_s} \times m_t \left(\ddot{\vec{\rho}}_{G_t/G_s}\right)_{x_s y_s z_s} \\
&\quad + \left[\vec{\rho}_{G_t/G_s} \times m_t \left(\dot{\vec{\omega}}_s \times \vec{\rho}_{G_t/G_s}\right)\right]_{x_s y_s z_s} \\
&= m_t \vec{\rho}_{G_t/G_s} \times \left(\ddot{\vec{\rho}}_{G_t/G_s}\right)_{x_s y_s z_s} + m_t \left(\overline{\rho}\vec{\omega}_s\right)_{x_s y_s z_s} \\
&= m_t \vec{\rho}_{G_t/G_s} \times \left(\ddot{\vec{\rho}}_{G_t/G_s}\right)_{x_s y_s z_s} \\
&\quad + m_t \left[(\dot{\overline{\rho}})_{x_s y_s z_s} \vec{\omega}_s + \overline{\rho}\left(\dot{\vec{\omega}}_s\right)_{x_s y_s z_s}\right]
\end{aligned} \tag{11}$$

where the relative velocity $\vec{v}_{G_t/G_s}$ is calculated by the absolute derivative of the radius vector $\vec{\rho}_{G_t/G_s}$. The symmetric matrix $\overline{\rho}$ is introduced to simplify the calculation of the derivative by letting $\vec{\rho}_{G_t/G_s} = [\rho_1, \rho_2, \rho_3]$ [6]:

$$\overline{\rho} = \begin{bmatrix} \rho_2^2 + \rho_3^2 & -\rho_1\rho_2 & -\rho_1\rho_3 \\ -\rho_1\rho_2 & \rho_1^2 + \rho_3^2 & -\rho_2\rho_3 \\ -\rho_1\rho_3 & -\rho_2\rho_3 & \rho_1^2 + \rho_2^2 \end{bmatrix} \tag{12}$$

The derivative of the radius vector $\vec{\rho}_{G_t/G_s}$ can be obtained from Eq. (8), which depends on the derivatives of various transformation matrixes. If the amplitude of the radius vector $\vec{\rho}_{G_t/G_s}$ is assumed to be constant, i.e. that the CM of the system is at a fixed point on a body, then the velocity and acceleration terms resulting from this vector, $(\ddot{\vec{\rho}}_{G_t/G_s})_{x_s y_s z_s}$ and $(\dot{\overline{\rho}})_{x_s y_s z_s}$, will disappear from Eq. (11), in which case this methodology degenerates to the specific case presented in [11]. The derivatives related to vectors $\vec{\rho}_{G_n/G_s}$ and $\vec{\rho}_{G_r/G_s}$ in Eq. (10) are calculated similarly. The introduction of the symmetric matrix ($\overline{\rho}$) facilitates the combination of similar terms from each rigid body and the separation of rotational DOFs ($\vec{\omega}_s$) from cross product terms. These separation enables numerical integration of the rotational EOMs using the efficient matrix form, typically used for solution of linear EOMs.

3.2. Translational equations of motion

Similar to the rotational EOMs, the conservation of linear momentum is applied to the entire wind turbine system directly, which eliminates the need to calculate internal forces between rigid bodies:

$$\sum \vec{F} = m_s \vec{a}_{G_s} \tag{13}$$

where $\vec{a}_{G_s}$ is the linear acceleration of the CM of the system, $\vec{a}_{G_s} = [\ddot{X}_1, \ddot{X}_2, \ddot{X}_3]$; m_s is the mass of the whole system, $m_s = m_t + m_n + m_r$; the force vector $\sum \vec{F}$ represents the external forces of the entire system in the inertia coordinate system (X, Y, Z), including environmental forces, restoring forces and gravity: $\sum \vec{F} = \vec{F}_{wind} + \vec{F}_{wave} + \vec{F}_{restoring} + \vec{G}$. Each of these components must be decomposed into the inertial coordinate system (X, Y, Z) for the application of Newton's second law. Restoring forces, $\vec{F}_{restoring}$, include contributions from buoyancy of the hull and tension of the mooring lines. The solution to this set of 3 translational EOMs is the motion of the CM of the multibody system measured from the (X, Y, Z) coordinate system. This CM is a mathematical convenience, the position of which may be continuously changing relative to both the (X, Y, Z) system and any of the three bodies making up the wind turbine model. The spatial position of the CM of the tower relative to G_s can be expressed as:

$$\vec{\rho}^{\,I}_{G_t/O} = \vec{\rho}^{\,I}_{G_s/O} + T_{s\to I}\vec{\rho}_{G_t/G_s} \tag{14}$$

where the radius vectors $\vec{\rho}^{\,I}_{G_s/O}$ and $\vec{\rho}_{G_t/G_s}$ result from the double integration of Eq. (13) and from Eq. (8), respectively; the transformation matrix from (x_s, y_s, z_s) to (X, Y, Z) can be expressed as:

$$T_{s\to I} = T_x(X_4)T_y(X_5)T_z(X_6) = \begin{bmatrix} t_{11} & t_{12} & t_{13} \\ t_{21} & t_{22} & t_{23} \\ t_{31} & t_{32} & t_{33} \end{bmatrix} \tag{15}$$

in which

$$\begin{aligned}
t_{11} &= \cos X_5 \cos X_6 \\
t_{12} &= -\cos X_5 \sin X_6 \\
t_{13} &= \sin X_5 \\
t_{21} &= \cos X_4 \sin X_6 + \cos X_6 \sin X_4 \sin X_5 \\
t_{22} &= \cos X_4 \cos X_6 - \sin X_4 \sin X_5 \sin X_6 \\
t_{23} &= -\cos X_5 \sin X_4 \\
t_{31} &= \sin X_4 \sin X_6 - \cos X_4 \cos X_6 \sin X_5 \\
t_{32} &= \cos X_6 \sin X_4 + \cos X_4 \sin X_5 \sin X_6 \\
t_{33} &= \cos X_4 \cos X_5
\end{aligned}$$

where $T_x(X_4)$, $T_y(X_5)$ and $T_z(X_6)$ are element transformation matrices [14]. The translational DOFs of the tower are defined as the motion of G_t measured from the (X, Y, Z) system, i.e. $\vec{\rho}^{\,I}_{G_t/O} = [X_{1t}, X_{2t}, X_{3t}]$, which is specified as the initial condition of translation and transferred to that of G_s by Eq. (14) for numerical integration of the translational EOMs. Similarly, the motion of G_s from Eq. (13) is transferred

to that of G_t, G_n and G_r for the calculation of external forcing at each time step.

4. External forcing

The external forcing (including both the external forces and moments) is composed of restoring forcing from hydrostatics and mooring lines as well as the environmental forcing due to wind and waves. The left hand side of the rotational EOMs (Eq. (1)) is the sum of the external moments in the translating-rotating system (x_s, y_s, z_s); the left hand side of the translational EOMs (Eq. (13)) is the external forces in the inertial system (X, Y, Z).

4.1. Restoring forcing

The large-amplitude motion of the wind turbine system results in nonlinear restoring forcing, which cannot be calculated by the conventional linear stiffness matrix method [11]. Here, the hydrostatic restoring forcing is calculated directly from the instantaneous buoyancy and the buoyancy center of the floater, which are nonlinear for large-amplitude motions. The floater (Fig. 1) includes two cylinders: a small surface-piercing cylinder and a larger subsurface cylinder connected by a tapered structural cone. Motions are assumed to be sufficiently small that the lower cylinder and taper remain fully submerged at all times and therefore have constant buoyancy and a fixed buoyancy center. The buoyancy and buoyancy center of the surface-piercing cylinder change with position of the cylinder. The instantaneous buoyancy and buoyancy center of the moving floater can be obtained by combining the two sets of forces and centers.

The instantaneous buoyancy of the surface-piercing cylinder in the inertial coordinate system, (X, Y, Z), is $\vec{F}^I_B = (0, 0, \rho g \pi r^2 h_1)$ [15], where ρ is the density of sea water; g is the gravitational acceleration; r is the radius of the cylinder; h_1 is instantaneous submerged length of the cylinder along the centerline. This variable length can be shown to be a function of heave motion and leaning angle of the cylinder:

$$h_1 = \frac{\rho_{G_M/G_t} - X_{3t}}{\cos\theta_1} - \rho_{G_M/G_t} + h_0 \tag{16}$$

where ρ_{G_M/G_t} is the distance measured from still water level to the CM of the tower in its equilibrium position; θ_1 is the leaning angle of the cylinder from vertical, $\cos\theta_1 = \cos X_4 \cos X_5$; h_0 is the initial length of h_1, i.e. the draft of the cylinder at equilibrium. Hydrostatic forces associated with waves above the mean still-water level are neglected in this formulation, as is common practice in naval architecture.

The variable center of buoyancy of this partially submerged cylinder piercing the water surface at an angle is described by the radius vector in the (x_t, y_t, z_t) system [15]:

$$\begin{aligned} \vec{\rho}_{B/G_t} &= (x_t^B, y_t^B, z_t^B) \\ x_t^B &= -\frac{t_{31} r^2}{4 t_{33} h_1} \\ y_t^B &= -\frac{t_{32} r^2}{4 t_{33} h_1} \\ z_t^B &= \vec{h}_G + \frac{h_1}{2} + \frac{r^2\left(t_{31}^2 + t_{32}^2\right)}{8 t_{33}^2 h_1} \end{aligned} \tag{17}$$

where the vector $\vec{h}_G$ indicates the position of the bottom of the surface-piercing cylinder (the top of the taper) measured from the (x_t, y_t, z_t) system along the centerline. The hydrostatic restoring moment from the cylinder can be expressed as $\vec{M}^s_B = \vec{\rho}_{B/G_s} \times (T_{I\to s} \vec{F}^I_B)$, in which the radius vector $\vec{\rho}_{B/G_s}$ can be calculated as $\vec{\rho}_{B/G_s} = \vec{\rho}_{B/G_t} + \vec{\rho}_{G_t/G_s}$. This moment is decomposed into the translating-rotating system, (x_s, y_s, z_s), consistent with the inertial forcing in the right hand side of Eq. (1). The restoring forcing from the fully submerged part of the floater (taper and lower cylinder) is combined with the contribution from surface-piercing cylinder to determine the total hydrostatic force.

A simplified mooring system is assumed for convenience, consisting of four radial taut lines. Compliance along each straight line is due to elasticity of the materials only, so the change in tension in each line is expressed as a function of cable stretch. Each fairlead position is calculated by summing the translational DOFs of the tower and the translations of the fair lead caused by the Euler angle rotations. This simplified mooring model neglects cable sag and mooring line dynamics, which could be important considerations for relatively small floaters such as wind turbines.

The radius position of any one fairlead (point A) in the inertia coordinate system (X, Y, Z) is $\vec{\rho}_{A/O} = \vec{\rho}_{G_t/O} + T_{t\to I} \vec{\rho}_{A/G_t}$, where the radius vector $\vec{\rho}_{G_t/O}$ results from Eq. (14); $\vec{\rho}_{A/G_t}$ is the radius position of point A in the (x_t, y_t, z_t) system; the transformation matrix $T_{t\to I}$ can be determined by Eq. (15). The position of the fixed end (point E) of this mooring line on the sea bottom, $\vec{\rho}_{E/O}$, is constant in the (X, Y, Z) system. Combining the radius position from point A to point E in the (X, Y, Z) system is $\vec{\rho}_{E/A} = \vec{\rho}_{E/O} - \vec{\rho}_{A/O}$. The tension along a neutrally buoyant taut line in the (X, Y, Z) system results from elasticity [15]:

$$\vec{F}^I_{line} = \left[T_0 + \frac{ES}{L}(\rho_{E/A} - L)\right] \frac{\vec{\rho}_{E/A}}{\rho_{E/A}} \tag{18}$$

where T_0 is the pretension of one mooring line; E is Young's Modulus; S is the cross sectional area of the line; L is the initial length of the line and $\rho_{E/A}$ is the norm of the vector $\vec{\rho}_{E/A}$, i.e. the instantaneous length of the line. The restoring force of the mooring system is obtained by summing the force from each line. Similarly, the restoring moment from each line in the (x_s, y_s, z_s) system is summed to obtain the contribution from the entire mooring system [11].

4.2. Environmental forcing

The wind force in the (X, Y, Z) system and wind moment calculated about G_s in the (x_s, y_s, z_s) system are applied in the EOMs of the system. For simplicity, an approximate wind thrust force is computed for the complete swept area of the blades following the method of Nielsen and Hanson [16]:

$$F_{thrust} = \frac{1}{2} C_T \rho_a A_b V_{yr}^2 \tag{19}$$

where ρ_a is the density of air; A_b is the swept area of the blades; C_T is the thrust coefficient; V_{yr} is the amplitude of the velocity of the wind relative to that of G_r along the y_r-axis. The wind force is assumed to be applied on the center of the blade area (G_r in Fig. 1) and along the y_r-axis, i.e. perpendicular to the swept blade area. The thrust coefficient, C_T, depends solely on relative wind velocity and is taken directly from Nielsen and Hanson [16] and repeated in Fig. 3. This curve is a proxy for the influence of conventional blade-pitch control on thrust. The curve was developed by assuming that the control mechanism maximizes the power output for wind speeds below the rated speed (17 m/s here) and retains constant power output after the rated speed. More accurate wind forces could be computed by linking the codes of this method with an existing rotor-aerodynamics module, e.g. AeroDyn [17].

The amplitude of relative velocity, V_{yr}, is computed by projecting both the wind velocity and structural velocity onto the Y_r-axis as $V_{yr} = \vec{V}^I_{wind} \cdot \vec{u}^I_y r - \vec{V}^I_{G_r} \cdot \vec{u}^I_y r$, in which $\vec{V}^I_{wind}$ is the wind velocity measured from the (X, Y, Z) system. The structural velocity of the center of the blade area can be expressed as: $\vec{V}^I_{G_r} = [\dot{X}_1\ \dot{X}_2\ \dot{X}_3]^T + T_{s\to I} \vec{v}_{G_r/G_s}$, where the relative velocity $\vec{v}_{G_r/G_s}$ can be obtained in a similar form to Eq. (11). The unit vector $\vec{u}^I_y r$ indicates the direction of the Y_r-axis in the (X, Y, Z) system by $\vec{u}^I_y r = T_{r\to I} \vec{u}^r_y r$, where $\vec{u}^r_y r$ is the unit

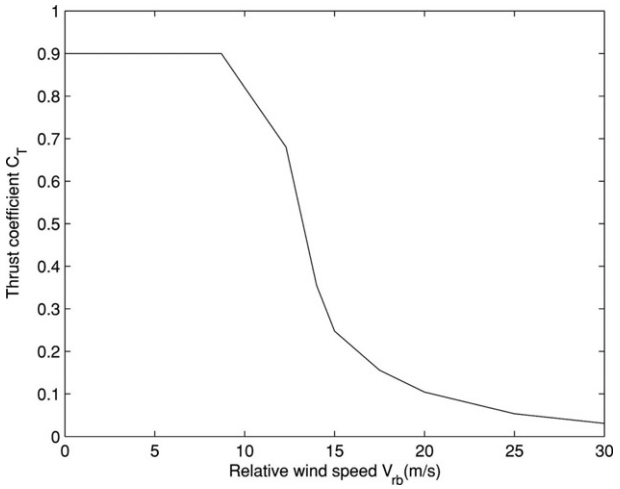

Fig. 3. Thrust coefficient as a function of relative wind velocity [16].

vector along Y_r-axis in the (x_r, y_r, z_r) system, i.e. $\vec{u}^r_y r = (0, 1, 0)$. The transformation matrix from (x_r, y_r, z_r) to (X, Y, Z), $T_{r\to I}$, is obtained by multiplication of the transformation matrix: $T_{r\to I} = T_{s\to I} T_{r\to s}$.

Finally, the wind force in the (X, Y, Z) system and the wind moment in the (x_s, y_s, z_s) system are:

$$\vec{F}_{wind} = T_{r\to I}\vec{F}^r_{wind} \tag{20}$$

$$\vec{M}_{wind} = \vec{\rho}_{G_r/G_s} \times \vec{F}^r_{wind} \tag{21}$$

where $\vec{F}^r_{wind}$ is the wind force in the (x_r, y_r, z_r) system: $\vec{F}^r_{wind} = (0, -F_{thrust}, 0)$. The aerodynamic torque is modeled as a constant equal to rated power divided by rotor speed, which is added to the wind moment.

The generalized Morison equation is used to calculate the wave forces per unit length normal to the axis of the leaning cylinder Sarpkaya and Issacson [18]:

$$\vec{f}^I_n = C_m\rho\frac{\pi}{4}D^2\dot{\vec{V}}_n - C_a\rho\frac{\pi}{4}D^2\dot{\vec{V}}_t + \frac{1}{2}\rho C_d D\vec{V}_{rt}\left|\vec{V}_{rt}\right| \tag{22}$$

where ρ is the density of sea water; D is the local diameter of the hull; C_m is the inertia coefficient; C_a is the added mass coefficient, and C_d is the drag coefficient. All velocities and accelerations are normal to the central axis of the tower: $\dot{\vec{V}}_n$ is the normal component of wave acceleration; $\dot{\vec{V}}_t$ is the normal component of structural acceleration; $\vec{V}_{rt}$ is the normal velocity of the water particle relative to the cylinder. The term associated with C_a in Eq. (22) is usually considered as the added mass. Viscous damping is included considering the relative velocity in the drag force calculation. The motions of the cylinder used in computing $\dot{\vec{V}}_t$ and $\vec{V}_{rt}$ result from solution of the equations of motion of the system (Eqs. (1) and (13)) from the prior time-step. As such, this generalized Morison formulation can be applied to compute the hydrodynamic forcing including structural motions and irregular seas without needing to impose assumptions beyond those already associated with a generalized Morison formulation. Use of the Morison equation implicitly assumes the body has a negligible effect on the incident waves, which is reasonable here because the hull structure is relatively slender. Dynamic pressure forces along the axis of the cylinder are also neglected, as is conventional for use of the Morison formulation; this assumption effectively neglects any changes to the buoyant force associated with passing waves (i.e., additional submerged volume due to passing wave peaks).

A unit vector along the central axis of the tower is needed in the (X, Y, Z) system to define the normal direction of kinematic vectors, $\vec{e}^I_3 = T_{s\to I}\vec{e}^t_3$, where $\vec{e}^t_3$ is a unit vector along centerline of the tower, $\vec{e}^t_3 = (0, 0, 1)$, in the (x_t, y_t, z_t) system. The normal component of water particle acceleration can be expressed as: $\dot{\vec{V}}_n = \vec{e}^I_3 \times (\dot{\vec{V}} \times \vec{e}^I_3)$, where $\dot{\vec{V}}$ is the wave acceleration vector in the (X, Y, Z) system. The structural velocity and acceleration of the segment along the tower can be obtained by the kinematics of rigid body:

$$\vec{V}_t = \vec{V}_{G_t} + T_{s\to I}\left(\vec{\omega}_t \times \vec{\rho}_{i/G_t}\right) \tag{23}$$

$$\dot{\vec{V}}_t = \vec{a}_{G_t} + T_{s\to I}\left[\dot{\vec{\omega}}_t \times \vec{\rho}_{i/G_t} + \vec{\omega}_t \times \left(\vec{\omega}_t \times \vec{\rho}_{i/G_t}\right)\right] \tag{24}$$

where $\vec{V}_{G_t}$ and $\vec{a}_{G_t}$ are the linear velocity and acceleration of the CM of the tower, G_t, in the inertial coordinate system (X, Y, Z); $\vec{\rho}_{i/G_t}$ is the vector radius from G_t to the segment with unit length. The wave kinematic velocity relative to the moving tower, $\vec{V}_{rt}$, is expressed as: $\vec{V}_{rt} = \vec{e}^I_3 \times (\vec{V}_r \times \vec{e}^I_3)$, where $\vec{V}_r$ is the relative velocity of the wave to the segment of the submerged tower: $\vec{V}_r = \vec{V} - \vec{V}_t$, in which $\vec{V}$ is the wave kinematic velocity in the (X, Y, Z) system. The wave force on the cylinder, $\vec{F}_{wave}$, is obtained by summing the force on each segment from Eq. (22). The wave moment in the (x_s, y_s, z_s) coordinate system can be computed by transforming the resulting forces from Eq. (22) into the (x_s, y_s, z_s) system and then numerically integrating over the submerged length of the tower.

$$\vec{F}_{wave} = \int_r \vec{f}^I_n dr \tag{25}$$

$$\vec{M}_{wave} = \int_r \left(\vec{\rho}_{i/G_s} \times \vec{f}^s_n\right) dr \tag{26}$$

where $\vec{f}^s_n = T_{I\to s}\vec{f}^I_n$ and $\vec{\rho}_{i/G_s} = \vec{\rho}_{i/G_t} + \vec{\rho}_{G_t/G_s}$.

5. Example

A compliant floating wind turbine design is obtained by truncating the spar cylinder of the OC3-Hywind model [19] from from 120 m to 84.4 m, saving about 2000 tonnes, or about or about 27% in total weight. This reduction also reduces the available hydrostatic restoring moment and allows larger pitch angle. The OC3-Hywind numerical model is based on Statoil's original Hywind system, but was modified to support the NREL 5-MW wind turbine. The topsides (nacelle and rotor) of the truncated model are the same as that in the OC3-Hywind: the moment of inertia of nacelle about yaw axis is 2.61×10^6 kg m^2; the moment of inertia of rotor about spin axis is 3.54×10^7 kg m^2. The displaced volume of water is reduced from the original 8.03×10^3 m^3 to 5.56×10^3 m^3. The moments of inertia of the tower (including hull) are 5.85×10^9 kg m^2 and 1.12×10^8 kg m^2 in the tilt (roll and/or pitch) and yaw, respectively, in the (x_t, y_t, z_t) system originating at G_t. The four taught-leg mooring lines are each assumed to be a straight axial spring with stiffness of 6.81×10^5 N/m and length of 564-m in a 320-m water depth location. The origin of the global coordinate system (X, Y, Z) is the initial position of the CM of the tower, i.e. 58.67 m below still water level.

The truncated design is first used to verify the new method by comparison with the popular wind turbine dynamics software FAST [9] for a small-amplitude motion case. FAST has been previously validated for small-angle motions by comparison with measured data [20], and is believed to provide reasonable verification of the new methodology presented here. The same model is then applied to large-amplitude motion. Results for a previously investigated 2-body system [11], and for a 3-body system are critically compared to quantify the influence of including small changes to the position of the CM of the system (G_s) and changes to the inertia tensor caused by nacelle yaw. Finally,

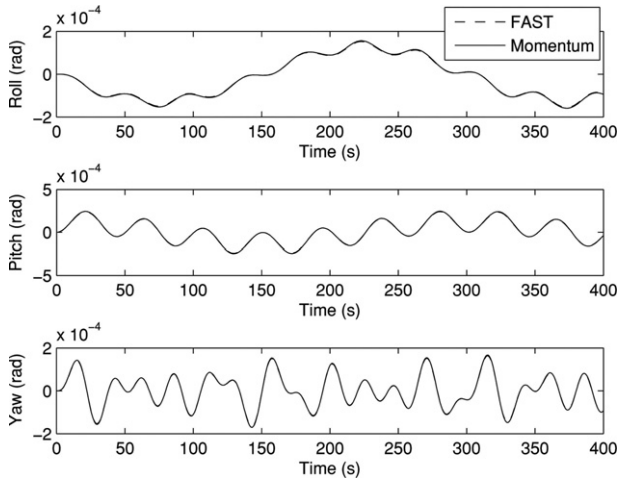

Fig. 4. Rotation verification for small-angle motion.

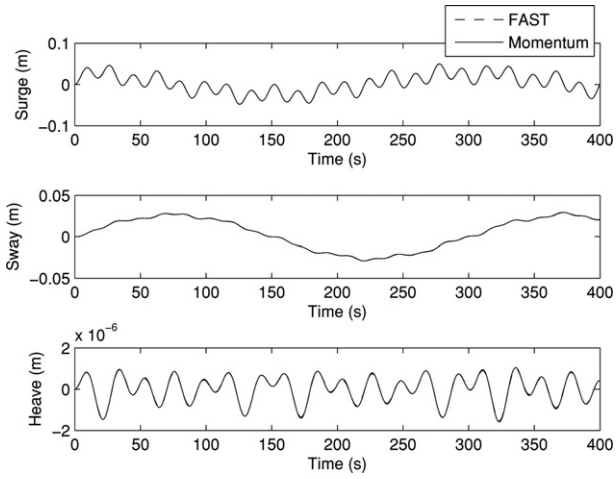

Fig. 5. Translation verification for small-angle motion.

the new method is applied to simulate the general motion of the compliant design subject to nacelle yaw associated with a rapid wind shift.

5.1. Free vibration verified by FAST

Figs. 4 and 5 show time histories computed using FAST and those computed using the conservation of momentum method for a small-amplitude free vibration case. The rotational DOFs of the tower are transferred to the inertial coordinate system used in FAST to enable direct comparison between (X_4, X_5, X_6) and pitch, roll and yaw, which is valid for small-amplitude rotation [21]. The translational DOFs, (X_{1t}, X_{2t}, X_{3t}), are transferred to the waterplane to enable direct comparison with the sway, surge and heave computed in FAST, which are measured from the (X_M, Y_M, Z_M) system in Fig. 1. Constant nacelle yaw (1.2°/s) and rotor spin (12.1 rpm) are prescribed during the simulation. To enable a direct comparison, hydrodynamics, aerodynamic forces and body flexibility have all been disabled in FAST and no results from WAMIT are used. The only external forces acting on the body are from the mooring lines and buoyancy, the combined restoring force from both hydrostatics and mooring are represented in the user-defined subroutine (UserPtfmLd) in FAST as a single 6×6 restoring matrix. The values used in this linear restoring matrix were developed to represent the non-linear restoring forces as closely as possible: First, the values in the matrix were computed using the methods presented in Section 4.1 for an average tilt angle; these linear approximations of the non-linear stiffness were then further refined by making small adjustments in the individual numerical entries in the matrix until the observed natural frequencies computed by each of the two methods were in good agreement. In the simulations, the initial conditions of six DOFs of tower motion are zero. The CM of the nacelle is not directly above the axis of the tower, so nacelle yaw motion changes the position of the CM of the system relative to the tower, which causes the tower motion. Figs. 4 and 5 show that the global motions of FAST and the momentum method are virtually indistinguishable. The spin axis is initially parallel to the surge direction. The influence of the moving G_s is clearly observable in the coupled motion of translational and rotational moving DOFs. For example, both pitch and surge are minimized (zero crossing) when the nacelle yaw angle is 90° (at 75 s), while roll and sway are maximized. The observed yaw motion results from gyro moments associated with rotor spin coupled with roll and pitch.

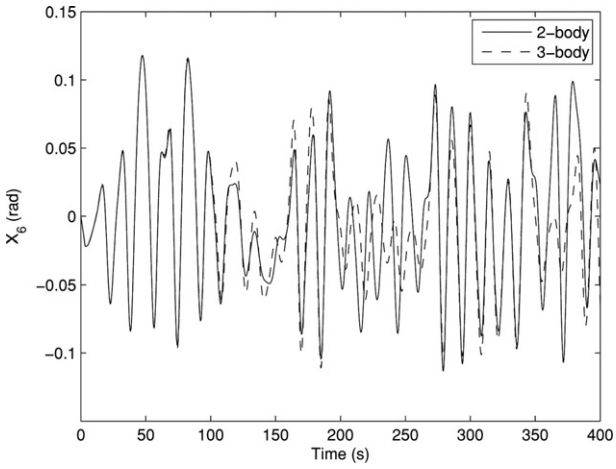

Fig. 6. Rotational motion: 2-body vs 3-body models.

5.2. Effect of a variable center of mass on free vibration

Figs. 6 and 7 show the comparison of global motion between the 2-body [11] and 3-body systems using the same truncated model. As in the prior example, this is a free-vibration case in which the only externally applied forces are the restoring forces from the mooring lines and hydrostatics. The large-amplitude initial conditions are prescribed to be $X_4 = X_5 = 0.4$ rad. Constant nacelle yaw (0.3°/s) and rotor spin (12.1 rpm) are also prescribed. Figs. 6 and 7 show the significant influence of the unconstrained G_s on the global motion (only X_6 and X_{3t} shown). In the 2-body system, the CM of the system (G_s) is constrained to the tower axis and independent of nacelle yaw, because the 2-body representation requires that the radius vector from G_s to the CM of each body (e.g. $\vec{\rho}_{G_t/G_s}$) remains constant. However, the more accurate modeling of the 3-body system enables correct calculation of changes to the CM of G_s and therefore changes to the inertia tensor associated with nacelle yaw. The effect is that the 3-body model includes changes to both the angular momentum and external moments in rotational EOMs (Eq. (1)) associated with the change of reference point G_s at each time step, which results in significant differences in computed rotation about the tower axis (Fig. 6).

Accurate simulation of the unconstrained G_s has a similar effect on vertical motion. The moving G_s is captured by Eq. (14) and coupled with the roll and pitch motions of the tower, the effect of which is to change the vertical motion of G_t (X_{3t}). In a separate simulation, the

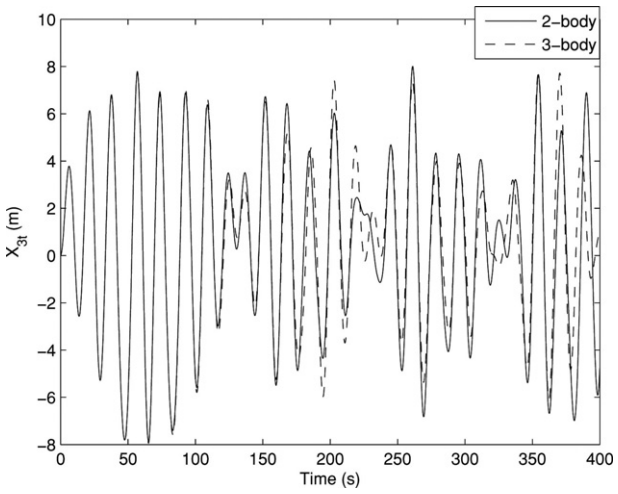

Fig. 7. Translational motion: 2-body vs 3-body models.

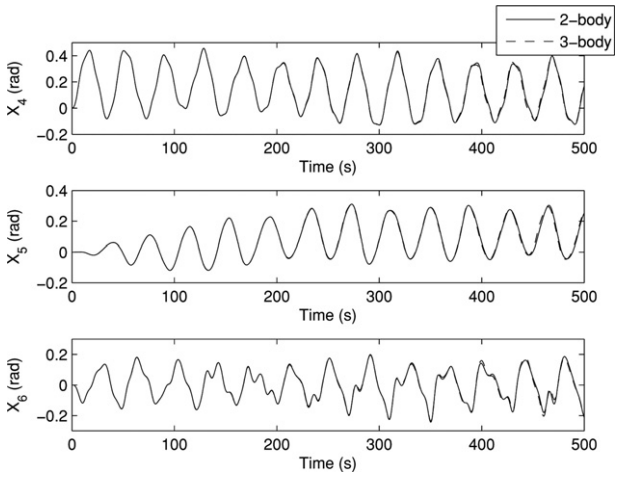

Fig. 8. Rotation with variable thrust coefficient: 2-body vs 3-body models.

overhang length of the rotor in the 3-body system was adjusted to make the CM of the topsides exactly on the top of the tower, such that the 3-body system effectively degenerates to the 2-body system. In this case, the general motion of the 3-body system matched the 2-body system perfectly (plot of results not shown).

5.3. Forced vibration with nacelle yaw

Figs. 8–10 show global motion for the same compliant spar model subject to realistic environmental forcing. The mean wind velocity at hub height is 18.2 m/s. Irregular wind velocities are simulated using TurbSim [22]. The wave environment is represented by a JONSWAP spectrum with a significant wave height of 5.0 m and peak period of 10 sec. The wind is along the negative direction of the *Y*-axis during the first 100 s and then suddenly shifts by $\pi/4$ rad towards the negative *X* direction in the *XOY* plane. The wind shift causes the nacelle yaw control to activate at 100 s, yaw the nacelle at a constant 0.3°/s, and then deactivate at around 250 s. Wave forces are computed using the Morison equation from a first-order time-domain representation of irregular waves simulated directly from the wave spectrum using a uniform phase distribution. The inertia coefficient C_m in Eq. (22) is assumed to be 2.0; the added mass coefficient C_a is assumed to be 1.0; the drag coefficient C_d is assumed to be 0.6. Fig. 8 shows simulation results of 1-2-3 sequenced Euler angles, in which wind forces are computed using the variable thrust coefficient based on Fig. 3. Fig. 9 shows the associated motion of G_t measured from the global coordinate system (*X*, *Y*, *Z*). The nonzero means of X_4 and X_{3t} indicate that the tower is always leaning away from the wind. The change in the mean of X_5 from zero to nonzero is due to the wind shift. Figs. 8 and 9 also compare the response computed using the 2- and 3-body models subject to identical environmental forcing. Visible differences in the response appear only late in the 500-second time-history, indicating that for this case of realistic environmental forcing it is a reasonable assumption to effectively constrain G_s to a fixed point on the tower. Fig. 10 shows the results of a simulation in which wind forces are computed using a fixed thrust coefficient of $C_T = 0.15$ in Eq. (19). Both the sway of G_s (X_1) and roll of the tower (X_5) clearly show the transition of mean between 100 s and 250 s. The positive damping introduced by fixed thrust coefficient decreases both the maxima and the envelope of the motion considerably, as was previously noted by Nielsen and Hanson [16].

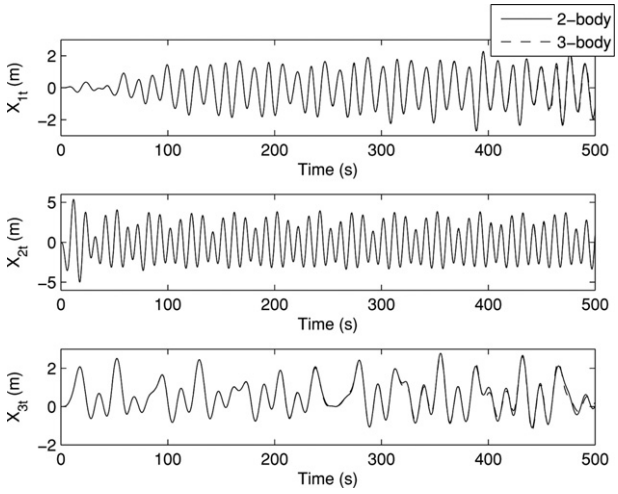

Fig. 9. Translation with variable thrust coefficient: 2-body vs 3-body models.

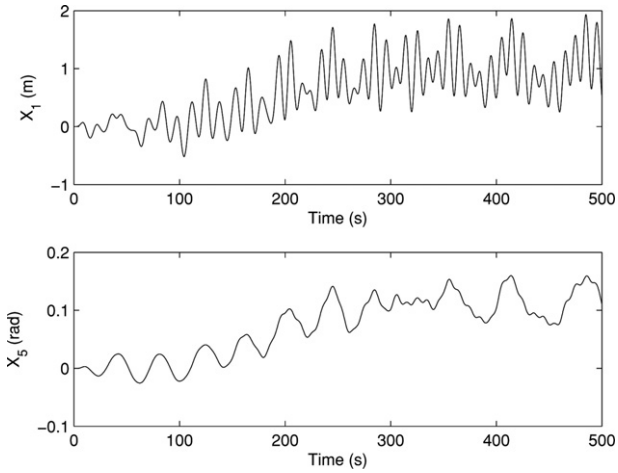

Fig. 10. Motion with fixed thrust coefficient.

6. Conclusions

A new formulation of multibody dynamics has been developed to directly apply the conservation of angular momentum to a 3-body representation of an entire compliant floating wind turbine system

including tower, rotor and nacelle. The formulation includes recomputing the unconstrained CM of the system as it moves due to relative motion among the rigid bodies. The inertial coupling between translational and rotational EOMs is eliminated by prescribing the translation and rotation of the base body as the six basic DOFs. Thus, motions of an 8-DOF system are represented as six basic EOMs plus two explicit control equations. The 1-2-3 sequence Euler angles are applied to describe the large-amplitude rotation of the tower, and transformation matrixes between various coordinate systems are developed. The restoring forcing and environmental forcing are calculated including full consideration of the nonlinear coupling among translational and rotational DOFs. Motions and external forcing are both transformed between the different coordinate systems at each time step such that the fully nonlinear coupling between external forcing and large-amplitude motion of the system is preserved. The new method is verified for small-amplitude motion by comparison with the well-known software FAST. Comparison of motions between a previously developed 2-body system [11] and 3-body system is shown to quantify the influence of including the effect of accurately calculating the unconstrained CM of the system. The new method is also used to simulate the general motion of the compliant design subject to nacelle yaw. A major strength of this new method is that it can be readily expanded to represent a wind turbine system using a greater number of rigid bodies.

Acknowledgements

This work was supported by the National Science Foundation, Energy for Sustainability within the Division of Chemical Bioengineering, Environmental and Transport Systems, agreement number CBET-1133682. Any opinions, findings, and conclusions or recommendations expressed in this material are those of the authors and do not necessarily reflect the view of the National Science Foundation.

References

[1] Henderson AR, Vugts JH. Prospects for floating offshore wind energy. In: Proceedings of the European wind energy conference. 2001, pp. 1–5.
[2] Wang L, Sweetman B. Conceptual design of floating wind turbines with large-amplitude motion. In: The proceedings of society of naval architects and marine engineers. SNAME. 2011, pp. 58–67.
[3] Saha S. Dynamics of serial multibody systems using the decoupled natural orthogonal complement matrices. Journal of Applied Mechanics 1999;66(4):986–96.
[4] Featherstone R. Rigid body dynamics algorithms. Springer, New York; 2008.
[5] Mason MT. Mechanics of robotic manipulation. MIT Press, Cambridge, MA; 2001.
[6] Stoneking E. Newton–Euler dynamic equations of motion for a multibody spacecraft. In: AIAA guidance, navigation, and control conference. 2007, pp. 1368–80.
[7] Matsukuma H, Utsunomiya T. Motion analysis of a floating offshore wind turbine considering rotor-rotation. The IES Journal Part A: Civil and Structural Engineering 2008;1(4):268–79.
[8] Jonkman JM, Buhl MLJ. FAST user's guide. Tech. Rep. NREL/EL-500–38230. National Renewable Energy Laboratory; 2005.
[9] Jonkman JM. Dynamic modeling and loads analysis of an offshore floating wind turbine.Tech. Rep. NREL/TP-500–41958. NREL National Energy Renewal Laboratory; 2007.
[10] WAMIT 6.4. WAMIT: the state of the art in wave interaction analysis – user manual. Dept. of Ocean Engineering, M.I.T.; 2008.
[11] Wang L, Sweetman B. Simulation of large-amplitude motion of floating wind turbines using conservation of momentum. Journal of Ocean Engineering 2012;42C:155–64.
[12] Hibbeler RC. Engineering mechanics – statics and dynamics. Pearson Prentice Hall, Upper Saddle River, NJ; 2004.
[13] Eberly D. Euler angle formulas. Tech. Rep. Geometric Tools, LLC; 2008 http://www.geometrictools.com/.
[14] Sweetman B, Wang L. Large-angle rigid body dynamics of a floating offshore wind turbine using euler's equations of motion. In: NSF CMMI research and innovation conference: engineering for sustainability and prosperity. 2011.
[15] Zeng XH, Shen XP. Nonlinear dynamics response of floating circular cylinder with taut tether. In: Proceedings of fifteenth offshore and polar engineering conference. 2005, pp. 218–24.
[16] Nielsen FG, Hanson TD, Skaare B. Integrated dynamic analysis of floating offshore wind turbines. In: Proceedings of the international conference on offshore mechanics and arctic engineering. 2006.
[17] Laino DJ, Hansen AC. User's guide to the wind turbine aerodynamics computer software AeroDyn. Tech. Rep.. National Energy Renewal Laboratory; 2011 http://wind.nrel.gov/designcodes/simulators/aerodyn/.
[18] Sarpkaya T, Issacson M. Mechanics of wave forces on offshore structures. Van Nostrand Reinhold Company, New York; 1981.
[19] Jonkman J. Definition of the floating system for phase IV of OC3. Tech. Rep. NREL/TP-500-47535. NREL National Energy Renewal Laboratory; 2010.
[20] Stewart G, Lackner M. Calibration and validation of a fast floating wind turbine model of the deepcwind scaled tension-leg platform. Tech. Rep. NREL/CP-5000-54822. NREL National Energy Renewal Laboratory; 2012.
[21] Abkowitz MA. Stability and motion control of ocean vehicles. M.I.T. Press, Cambridge, MA; 1969.
[22] Kelley N, Jonkman B. NWTC design codes (TurbSim). Tech. Rep.. National Renewable Energy Lab; 2008 http://wind.nrel.gov/designcodes/.